THEORY FOR ALLOTRIOMORPHIC FERRITE FORMATION IN STEEL WELD DEPOSITS

H. K. D. H. Bhadeshia*, L. -E. Svensson** and B. Gretoft**

*University of Cambridge
Department of Materials Science and Metallurgy
Pembroke Street, Cambridge CB2 3QZ, U.K.
**ESAB AB, Gothenburg, Sweden

Abstract

Recent theoretical work has enabled the rationalisation and prediction of the primary microstructure of steel welds as a function of chemical composition, welding conditions and other variables. There are, however, systematic discrepancies in the estimation of the volume fraction of allotriomorphic ferrite. In this work, we present a detailed theoretical analysis of allotriomorphic ferrite formation, which avoids some of the approximations of the earlier method. The new theory accounts also for factors influencing the nucleation of ferrite, and hence can in principle be used for high-alloy welds and for welds containing boron as a minor addition. The results are compared (in a limited way) with some published experimental data.

Nomenclature

Throughout this work, braces are used exclusively to indicate functional relations. For example, D{x} implies that x is the argument of the function D.

a	Side-length of the cross-section of a hexagonal prism
c	Length of a hexagonal prism
D	Diffusivity of carbon in γ
$\overline{D}$	Weighted average diffusivity of carbon in γ
I_B	Grain boundary nucleation rate per unit area
O	Total area of a plane surface
O_b	Area of a particular grain boundary
O_B	Area of all grain boundaries
O_α^e	Extended area due to the intersection of an α allotriomorph with a test plane
O_α	Actual area due to intersection of an α allotriomorph with a test plane
q	Half thickness of an allotriomorph of ferrite
S_v	Grain boundary surface area per unit volume
T_h	Temperature at which γ first transforms to α during continuous cooling
T_l	Temperature at which $\gamma \rightarrow \alpha$ transformation stops during continuous cooling
t_s	Time at which soft impingment becomes significant
V_V^α	Volume fraction of α
V_α	Actual volume of α
V_α^e	Extended volume of α
$\overline{x}$	Average carbon content of alloy
$x^{\alpha\gamma}$	Equilibrium or paraequilibrium C content of α
$x^{\gamma\alpha}$	Equilibrium or paraequilibrium C content of γ
α	Allotriomorphic ferrite
α_a	Acicular ferrite
α_w	Widmanstätten ferrite
α_1	One-dimensional parabolic thickening rate constant
α_2	Parabolic thickening rate constant for oblate ellipsoid
δ	Delta-ferrite
γ	Austenite
η	Ratio of length to thickness of allotriomorph
τ	Incubation time for the nucleation of one particle
ϕ	Equilibrium volume fraction of α

Introduction

The primary microstructure of a weld is that part which is not influenced by any subsequent heat input. It consists of allotriomorphic ferrite (α), Widmanstätten ferrite (α_w), acicular ferrite (α_a) and "microphases" (i.e., small amounts of martensite, degenerate pearlite, retained austenite). Recent work (1-7) has enabled the estimation of the primary microstructure of steel weld deposits to a reasonable degree of accuracy.

All of the constituents of the primary microstructure are important in determining the properties of a weld deposit. One of the more important properties is toughness, and it is generally recognised that thick layers of allotriomorphic ferrite at the austenite grain boundaries are detrimental to toughness because they offer little resistance to cleavage crack propagation (8). It is therefore necessary to control carefully the volume fraction V_V^{α} of allotriomorphic ferrite. The theory (1-7) for the prediction of the allotriomorphic ferrite has a number of unsatisfactory approximations, whose significance can best be understood after discussing briefly the way in which microstructure is calculated (1-7):

(a) The input data for the calculations consist of chemical composition, which may include C, Si, Mn, Ni, Cr, Mo and V in any reasonable combination. A weld cooling curve, either measured or estimated (7) using heat-flow theory and welding parameters is also necessary. The austenite grains of welds can be represented (9) as a honeycomb of space-filling hexagonal prisms of length "c" and hexagon side-length "a"; since c>>a, and since the model ignores α formation on the ends of the hexagons, only the parameter "a" is needed as an input. This can either be measured or estimated empirically (7) as a function of chemical composition and heat-input.

(b) The chemical composition is used to calculate a paraequilibrium (10-12) phase diagram which includes the Ae3' $\alpha/\alpha+\gamma$ phase boundary, the T_0 curve, and the same curves after appropriate modifications for strain energy effects due to the displacive character of some of the phase transformations that arise in welds.

The Ae3' curve on a plot of temperature versus carbon concentration represents the *paraequilibrium* $\alpha/\alpha+\gamma$ phase boundary, where paraequilibrium is a form of constrained equilibrium in which substitutional atoms do not redistribute during transformation, but carbon partitions such that it has equal chemical potential in both phases at the interface. The T_0 curve on the same plot represents the locus of all points where α and γ of the same composition have equal free energy. Diffusionless transformation is thermodynamically possible only if the γ composition falls to the left of the T_0 curve.

The phase diagram is needed in order to calculate the compositions at the α/γ interface during α growth, which is assumed to occur at a rate controlled by the diffusion of carbon in the γ ahead of the interface. Since the diffusivity D of carbon in γ is a function of its carbon concentration, a reliable method (13,14) of representing this function is necessary so that a weighted average diffusivity (15) $\bar{D}$ can be substituted for D in the rate equations. This is strictly justified only when growth occurs at a constant rate, but numerical calculations (3) have demonstrated the approximation is extremely good for typical weld deposits. Finally, the Ae1 curve, which represents the composition of α in equilibrium with γ is calculated, as a good approximation (since the carbon concentration of ferrite is very small) to the paraequilibrium Ae1' curve.

(c) Having calculated the phase diagram, an isothermal transformation (TTT) curve is also computed using methods described elsewhere (16). However, welds are known to be chemically heterogeneous and this can cause an underestimation in the calculated value of V_V^{α}. To allow for this, the weld is divided into solute-rich and solute-depleted regions (with respect to substitutional elements only, since C diffuses very rapidly so that its activity should become

uniform during cooling) (5). It is assumed that ferrite formation first begins (at a temperature T_h) in the solute-depleted regions, whose composition is calculated by computing the partition coefficients for substitutional elements, for partitioning between liquid and δ (it is solidification which gives rise to segregation in the first place). Thus, a new TTT curve is calculated for the solute-depleted region, and in combination with the weld cooling curve, can be used to compute T_h using an additive reaction rule (reviewed in ref.17), which treats continuous cooling as a series of short isothermal transformations, each occurring at a successively lower temperature until the transformation eventually stops at the temperature T_l. This is the temperature at which diffusional transformations become sluggish and give way to displacive reactions (e.g., α_w), when the diffusional C-curve of the TTT diagram crosses the displacive C-curve.

(d) The half-thickness q of the allotriomorph is calculated using the equation (1):

$$q = \int_{t=0}^{t_1} 0.5\alpha_1 t^{-0.5}\, dt \qquad (1)$$

where t=0 when the alloy reaches the temperature T_h, and $t=t_1$ at T_l. Note that α_1 is the one-dimensional parabolic thickening rate constant, and for continuous cooling transformation is a complicated function of temperature and hence of time; the equation is therefore numerically integrated. The analysis assumes that at T_h, the γ grain boundaries become decorated instantaneously with an infinitesimally thin layer of α, so that α formation is (below T_h) a growth problem involving the one-dimensional thickening of allotriomorphs.

(e) Having calculated q, V_V^α is given, from geometrical considerations by (1):

$$V_V^\alpha = 4qC_3(a - qC_3)/a^2 \qquad (2)$$

where $C_3=\tan\{30^o\}$.

This procedure works well if the calculated volume fraction is multiplied by a factor of about two (1); the theory *consistently* underestimates the amount of allotriomorphic ferrite. This is clearly not satisfactory, but is encouraging since the calculated volume fraction correlates extremely well (correlation coefficient typically 0.95) with the experimental data, and bearing in mind the factor of two, the model can, and is being used extensively in the design of weld deposits (18). In this work, we present new theory which should help eliminate many of the approximations made in the earlier model. The new theory is more general in the sense that it can also be applied to more heavily alloyed welds and to welds where α formation is nucleation limited.

Theory

It is believed that the major assumption (illustrated in Fig. 1) in our earlier model, which causes a consistent underestimation of V_V^α, is that at T_h the γ boundaries become decorated uniformly with a thin layer of α, the α subsequently thickening normal to the γ grain boundary. In some heavily alloyed welds this is unjustified since discontinuous layers of α are observed (3). Even when uniform and continuous layers of α are observed, the early stages must involve a faster rate of transformation since growth is initially not confined to one dimension. It is only when site-saturation occurs that one-dimensional allotriomorph thickening should be a good approximation.

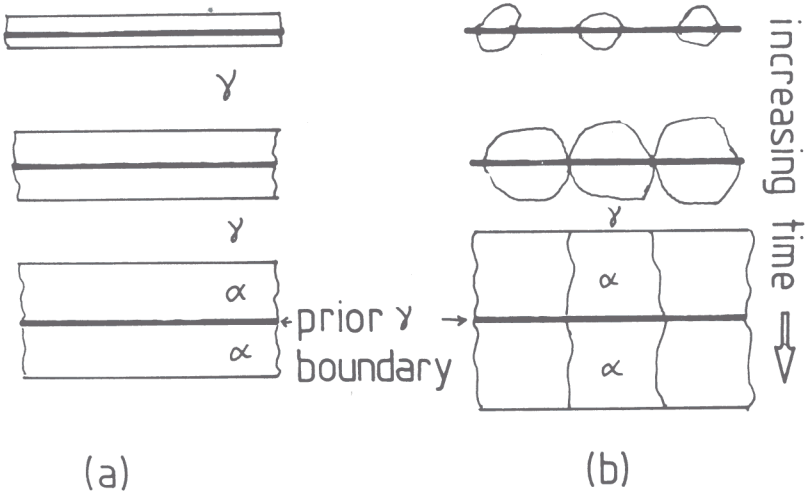

Figure 1 - Diagram illustrating allotriomorphic ferrite as theoretially modelled (a), and as is the case in reality (b).

Allotriomorphs as discs

The allotriomorphs prior to site-saturation are modelled as discs parallel to the austenite grain boundary planes, of half-thickness q, radius ηq. An analysis will also be presented for allotriomorphs with are oblate ellipsoids, but for reasons discussed later, the disc model is probably a better approximation. The aspect ratio η of the allotriomorphs is considered constant because in reality, lengthening and thickening processes are coupled. The method takes account of hard impingement; the problem of soft-impingement is discussed later.

In the derivation that follows, we use the method of Cahn and Avrami (19,20), for the calculation of isothermal reaction kinetics for nuclei forming preferentially at grain boundary faces. Nucleation on grain edges and corners is ignored because the γ grain size for welds is large, and because ferrite formation in welds starts at relatively high supersaturations (1). Cahn's method is here modified for the parabolic growth kinetics of α. The general theory of overall transformation kinetics has been thoroughly reviewed by Christian (17), and for the sake of brevity, an understanding of the concept of extended area or volume is assumed.

Consider a plane surface of total area O parallel to a particular boundary; the extended area O^e_α is defined as the sum of the areas of intersection of the discs with this plane. It follows that the change dO^e_α in O^e_α due to disc nucleated between $t=\tau$ and $t=\tau+d\tau$ is:

$$dO^e_\alpha = \pi O_b I_B[(\eta\alpha_1)^2(t - \tau)]d\tau \qquad \text{for } \alpha_1(t - \tau)^{0.5} > y \tag{3}$$

and

$$dO^e_\alpha = 0 \qquad \text{for } \alpha_1(t - \tau)^{0.5} < y$$

where y is the distance between the boundary and an arbitrary plane parallel to the boundary.

Bearing in mind that only particles nucleated for $\tau > [(y/\alpha_1)^2]$ can contribute to the extended area intersected by the plane at y, the whole extended area is given by:

$$O^e_\alpha = \int_0^{t-(y/\alpha_1)^2} (\eta\alpha_1)^2\pi O_b I_B(t - \tau)d\tau$$

$$= 0.5\pi O_b I_B(\eta\alpha_1)^2 t^2[1 + \theta^4 - 2\theta^2] \tag{4}$$

Should be $[1 - \theta^4]$

where $\theta = y/(\alpha_1 t^{0.5})$.

Given that the relationship between extended area and actual area O_α is given by (17,19):

$$O^e_\alpha / O = -\ln\{1 - [O_\alpha / O]\} \tag{5}$$

and assuming that there is no interference with allotriomorphs from other boundaries, the total volume V_b of material originating from this grain boundary is given by integrating for all y between negative and positive infinity; in terms of θ, the integral amounts to:

$$V_b = \int_0^1 2O_b (\alpha_1 t^{0.5})(1-\exp\{-O^e_\alpha/O_b\}) \, d\theta$$

$$= \int_0^1 2O_b (\alpha_1 t^{0.5})(1-\exp\{-0.5\pi I_B(\eta\alpha_1)^2 t^2[1 - \theta^4]\}) \, d\theta$$

$$= 2O_b(\alpha_1 t^{0.5}) f\{\theta, \eta\alpha_1, I_B, t\}$$

where

$$f\{\theta, \eta\alpha_1, I_B, t\} = \int_0^1 (1-\exp\{-0.5\pi I_B(\eta\alpha_1)^2 t^2[1 - \theta^4]\}) \, d\theta \tag{6}$$

If the total grain boundary area is $O_B = \Sigma O_b$, then by substituting O_B for O_b in the above equation the total extended volume V^e_α of material emanating from all boundaries is found; this is an *extended* volume because allowance was not made for impingement of discs originating

from different boundaries. Thus,

$$V_\alpha^e = 2O_B(\alpha_1 t^{0.5})f\{\theta, \eta\alpha_1, I_B, t\}$$

and if V is the total volume, and S_v the γ grain surface area per unit volume, then:

$$V_\alpha^e / V = 2S_v(\alpha_1 t^{0.5})f\{\theta, \eta\alpha_1, I_B, t\}.$$

This can be converted into the actual volume V_α using the equation:

$$V_\alpha / (V\phi) = 1 - \exp\{-V_\alpha^e / (V\phi)\}$$

where $\phi = (x^{\gamma\alpha} - \bar{x})/(x^{\gamma\alpha} - x^{\alpha\gamma})$

It follows that:

$$-\ln\{1 - \zeta\} = (2S_v/\phi)(\alpha_1 t^{0.5})f\{\theta, \eta\alpha_1, I_B, t\} \quad (7)$$

where $\zeta = V_\alpha / (V\phi)$, i.e., it is the volume of α divided by its equilibrium volume.

Finally, it should be noted that the value of the integral f tends to unity as I_B increases or time increases, since site saturation occurs. In the limit that the integral is unity, eq.7 simplifies to one dimensional thickening as in the earlier model:

$$-\ln\{1 - \zeta\} = (2S_v / \phi)(\alpha_1 t^{0.5}) \quad (8)$$

Allotriomorphs as Oblate Ellipsoids

Obara *et al.* (21) have stated an equation for an oblate ellipsoid representation of allotriomorphs, although the derivation was not given and the factor ϕ was not included in their analysis. From geometrical considerations and by comparison with eq.3, it follows that for oblate ellipsoids, the change in the extended area at the plane located at distance y from the boundary, due to particles nucleated between $t=\tau$ and $t=\tau+d\tau$ is given by:

$$dO_\alpha^e = \pi O_b I_B[(\eta\alpha_2)^2(t - \tau)(1 - (y^2/(\alpha_2^2(t - \tau))))]d\tau \quad (9)$$

The function f is now replaced by the new function f_2 as follows:

$$f_2\{\theta, \eta\alpha_2, I_B, t\} = \int_0^1 (1-\exp\{-0.5\pi I_B(\eta\alpha_2)^2 t^2[1 - 2\theta^2 + \theta^4]\}) \, d\theta \quad (10)$$

where α_2 is the parabolic thickening rate constant for oblate ellipsoids; α_2 is in general larger than α_1. It follows that:

$$-\ln\{1 - \zeta\} = (2S_V / \phi)(\alpha_2 t^{0.5}) \; f_2\{\theta, \eta\alpha_2, I_B, t\} \qquad (11)$$

There is a disadvantage in using the oblate ellipsoid model for allotriomorphic ferrite formation in situations where site saturation occurs at an early stage of transformation, as is the case for welds. The oblate ellipsoid parabolic thickening rate constant α_2 only applies while the shape of the ferrite remains in the form of oblate ellipsoids. When the γ boundaries become decorated with α, the allotriomorphs grow in just one dimension, and at that stage, the one-dimensional parabolic thickening rate constant α_1 applies because the boundary conditions for the growth problem are then different.

Non-isothermal growth

The equations derived above may be used for the non-isothermal growth of ferrite in welds, if it is assumed that the reaction is isokinetic; this is probably a good assumption for welds since site-saturation occurs at an early stage of transformation.

The continuous cooling curve can then be divided into a series of isothermal steps. The procedure is not discussed here but has been reviewed by Christian (17).

Comparison with Experimental Data

The model derived above cannot be compared fully with experimental data; it is not possible to predict from first principles, the nucleation rate of ferrite.

It is however possible to test the *form* of the equations. For example, under both isothermal and non-isothermal conditions, if everything else is kept fixed, then $\ln\{1-\zeta\}$ should be directly proportional to S_V. Thewlis (22) has recently published a large amount of data (some 34 tandem submerged arc welds), which includes details on the austenite grain size, volume fractions of all the phases and chemical composition. The data can, for the present purposes be divided into two sets, one containing welds with negligible boron content, and another with welds containing about 30ppm by wt. of boron. These have to be treated separately since I_B should be much lower in the latter case; boron is known to reduce the austenite grain boundary energy by segregation (23), thereby causing an increase in the activation energy for heterogeneous nucleation.

The boron-free welds have a typical composition (wt.%) Fe-0.06C-0.25Si-1.37Mn-0.04V-0.11Mo, the other welds containing a slightly higher Mo concentration ($\approx$ 0.21 wt.%) and about 32 ppm by wt. of boron. Thewlis also tabulated mean lineal intercept ($\bar{L}$) measurements for γ grains; S_V may be derived from the stereological rule (24):

$$S_V = 2 / \bar{L} \qquad (12)$$

Because the chemical compositions of the welds in a given set are virtually identical, and since the same welding conditions are used for all welds, a plot of $\ln\{1-\zeta\}$ versus S_V should be

linear (even for non-isothermal conditions).

To obtain ζ, it is necessary to define ϕ, the equilibrium volume fraction of α. A phase diagram was calculated for each weld, taking into account the detailed composition of each weld, and ϕ was evaluated at the temperature T_1, where α formation ceases and gives way to more rapid displacive transformation. T_1 was determined from the calculated TTT curve for each weld, and the cooling curve was estimated using the welding conditions listed by Thewlis, and the heat flow parameters evaluated by Bhadeshia *et al.* (3)

A typical phase diagram and TTT curve is presented in Fig. 2. Fig. 3 shows that both sets of welds satisfy, to a reasonable degree, the linear relationship between $\ln\{1-\zeta\}$ and S_v, the scatter probably arising because: (a) the compositions of welds in each set are not strictly constant (Fe 0.05-0.07C 0.20-0.27Si 1.28-1.37Mn 0.09-0.15Mo 0.039-0.044V, wt. % for the boron free welds, and Fe 0.05-0.07C 0.20-0.27Si 1.36-1.42Mn 0.21-0.23Mo 0.038-0.044V wt.% for the other welds), (b) statistical error in the measurement of volume fraction.

Further testing of the theory requires a method for the reliable estimation of nucleation rates, and this is where our efforts will be concentrated in the future.

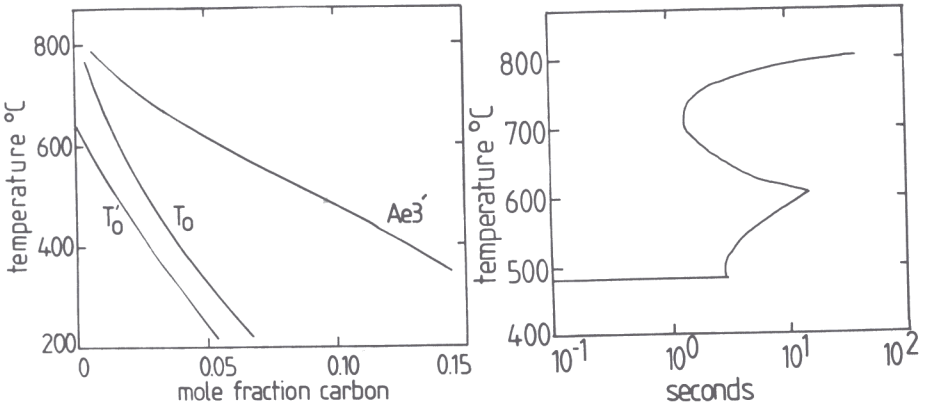

Figure 2 - Fe-0.06C-0.20Si-1.27Mn-0.041V-0.09Cr-0.11Mo-0.05Ni wt% alloy
(a) Calculated phase boundaries, (b) calculated TTT diagram.

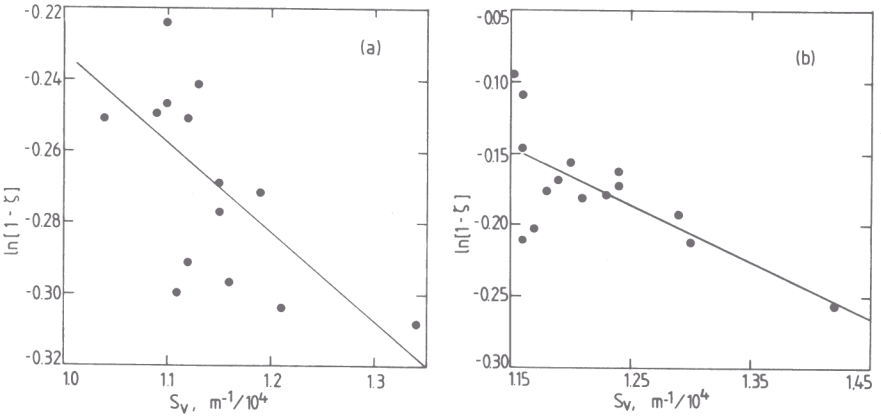

Figure 3 - Plots of $\ln\{1-\zeta\}$ versus S_v, as discussed in the text (data due to Thewlis). (a) Boron free welds, (b) boron containing welds.

Soft Impingement

Gilmour *et al.* (25) have treated the problem of soft impingement, i.e., the overlap of the diffusion fields of allotriomorphs growing from different boundaries. The diffusion profile ahead of the allotriomorph was approximated as being finite in extent, and soft impingement was considered to occur when the concentration at the end of the profile begins to rise above the average alloy carbon concentration. The time t_s before soft impingement is then given by:

$$t_s \approx (0.5a / \tan\{30^o\})^2 \, \bar{x} \, x^{\gamma\alpha} / [D\{x^{\gamma\alpha}\} \, (x^{\gamma\alpha} - \bar{x})] \qquad (13)$$

where we have taken the extent of the γ grain ahead of the grain boundary to be $(0.5a/\tan\{30^o\})$, consistent with the hexagonal prism γ grain morphology.

Typical calculations for t_s are given in Table 1; it is evident that for arc welds, where allotriomorphic ferrite formation is complete within a few seconds, soft impingement between allotriomorphs growing from opposite grain boundaries is not a problem.

Table 1: Some calculations of the time required for the onset of significant soft-impingement, using eq.13. The calculations are for the same alloy as in Fig. 2.

$x^{\gamma\alpha}$, mol. frac.	$D\{x^{\gamma\alpha}\}$, $cm^2/(10^{-8}s)$	t_s, s	Temp., ^oC
0.0004	1.470	5750	800
0.0113	0.926	2410	760
0.0196	0.591	1910	720
0.0303	0.389	1780	680
0.0435	0.255	1830	640
0.0521	0.140	2760	600

Conclusions

A new theory has been developed which allows the calculation of the volume fraction of allotriomorphic ferrite in welds, even when site saturation does not occur at an early stage of transformation. It has not been possible to fully test the model, since this awaits the development of at least a working hypothesis for the prediction of the nucleation rate of ferrite. However, it already provides an interpretation of effects such as the influence of austenite grain size on the volume fraction of ferrite. The model is incidentally, independent of the austenite grain shape, and as such should be applicable also to the heat-affected zone of welds or to the reheated microstructure of multipass welds.

Acknowledgments

The authors are grateful to ESAB AB for financial support and for the provision of laboratory facilities, and to Professor D. Hull for the provision of laboratory facilities at the University of Cambridge. Helpful discussions with A. A. B. Sugden are acknowledged with pleasure.

References

1. H. K. D. H. Bhadeshia, L.-E. Svensson and B. Gretoft,"A Model for the Development of Microstructure in Low-Alloy Steel Weld Deposits," Acta Metall., 33 (1985) 1271-1283.

2. H. K. D. H. Bhadeshia, L.-E. Svensson and B. Gretoft, "Prediction of the Microstructure of the Fusion Zone of Multicomponent Steel Weld Deposits," Trends in Welding Research, ed. S. A. David, (Metals Park, OH: American Society for Metals, 1987), 225-229.

3. H. K. D. H. Bhadeshia, L.-E. Svensson and B. Gretoft, "Prediction of the Microstructure of Submerged-Arc Linepipe Welds," Welding and Performance of Pipe Welds, (Welding Institute, Abington, Cambridge) in press.

4. L.-E. Svensson, B. Gretoft and H. K. D. H. Bhadeshia, "Computer-Aided Design of Electrodes for Manual Metal Arc Welding," Computer Technology in Welding, (Welding Institute, Abington, Cambridge), in press.

5. B. Gretoft, H. K. D. H. Bhadeshia and L.-E. Svensson, "Development of Microstructure in the Fusion Zone of Steel Weld Deposits," Acta Stereologica, 5 (1986) 365-371.

6. H. K. D. H. Bhadeshia, L.-E. Svensson and B. Gretoft, "The Influence of Alloying Elements on the Formation of Allotriomorphic Ferrite in Low-Alloy Steel Weld Deposits," J. Mat. Sci., 4 (1985) 305-308.

7. L.-E. Svensson, B. Gretoft and H. K. D. H. Bhadeshia, "An Analysis of Cooling Curves from the Fusion Zone of Steel Weld Deposits," Scand. J. of Metall., 15 (1986) 97-103.

8. J. H. Tweed and J. F. Knott, "Effect of Reheating on Microstructure and Toughness of C-Mn Weld Metal," Metal Science, 17 (1983) 45-53.

9. H. K. D. H. Bhadeshia, L.-E. Svensson and B. Gretoft, "The Austenite Grain Structure of Low-Alloy Steel Weld Deposits," J. Mat. Sci., 21 (1986) 3947-3951.

10. A. Hultgren, Jernkontorets Ann., 135 (1951) 403.

11. M. Hillert, Jernkontorets Ann., 136 (1951) 25.

12. H. K. D. H. Bhadeshia, "Diffusional Formation of Ferrite in Iron and its Alloys," Progress in Mat. Sci., 29 (1985) 321-386.

13. R. H. Siller and R. B. McLellan, "Application of First Order Mixing Statistics to the Variation of the Diffusivity of Carbon in Austenite," Metall. Trans., 1 (1970) 985-995.

14. H. K. D. H. Bhadeshia, "The Diffusion of Carbon in Austenite," Metal Science, 15 (1981) 477-479.

15. R. Trivedi and G. M. Pound, "Effect of Concentration-Dependent Diffusion Coefficient on the Migration of Interphase Boundaries,", J. Appl. Phys., 38 (1967) 3569-3576.

16. H. K. D. H. Bhadeshia, "A Thermodynamic Analysis of Isothermal Transformation Diagrams," Metal Science, 16 (1982) 159-165.

17. J. W. Christian, Theory of Transformations in Metals and Alloys, Part 1, 2nd Ed., (Oxford, Pergamon Press, 1975).

18. L.-E. Svensson, B. Gretoft and H. K. D. H. Bhadeshia, "Design of the Primary Microstructure of Arc Welds", Parts I-III, Internal Reports of ESAB AB and the University of Cambridge, 1986.

19. J. W. Cahn, "Kinetics of Grain Boundary Nucleated Reactions," Acta Metall., 4 (1956) 449.

20. M. Avrami, J. Chem. Phys., 7 (1939) 1103.

21. T. Obara et al., Solid→Solid Phase Transformations, (Metals Park, Ohio: American Society for Metals, 1981) 1105.

22. G. Thewlis, Welding and Performance of Pipe Welds, (Cambridge: Welding Institute 1986), in press.

23. F. B. Pickering, Phys. Metall. and the Design of Steels, (London: Applied Science Publishers, 1978), 104-5.

24. R. T. DeHoff and F. N. Rhines, Quantitative Microscopy, (New York: McGraw Hill, 1968).

25. J. B. Gilmour, G. R. Purdy and J. S. Kirkaldy, "Partition of Manganese During the Proeutectoid Ferrite Transformation in Steels," Metall. Trans. 3 (1972) 3213-3222.